

involve

a journal of mathematics

Weak and strong solutions
to the inverse-square brachistochrone problem
on circular and annular domains

Christopher Grimm and John A. Gemmer



Weak and strong solutions to the inverse-square brachistochrone problem on circular and annular domains

Christopher Grimm and John A. Gemmer

(Communicated by John Baxley)

In this paper we study the brachistochrone problem in an inverse-square gravitational field on the unit disk. We show that the time-optimal solutions consist of either smooth strong solutions to the Euler–Lagrange equation or weak solutions formed by appropriately patched together strong solutions. This combination of weak and strong solutions completely foliates the unit disk. We also consider the problem on annular domains and show that the time-optimal paths foliate the annulus. These foliations on the annular domains converge to the foliation on the unit disk in the limit of vanishing inner radius.

1. Introduction

In 1696 Johann Bernoulli posed the following problem: given two points A , B , find a curve connecting A and B such that a particle traveling from A to B under the influence of a uniform gravitational field takes the minimum time. This is called the *brachistochrone problem*, from the Greek terms *brachistos* for shortest and *chronos* for time. It was solved the following year by Leibniz, L'Hospital, Newton, and others [Dunham 1990]. While the solution to the brachistochrone problem has limited applications, the techniques from calculus used to solve it were novel at the time. Namely, rudimentary techniques from what would later be called the calculus of variations were developed. Euler and Lagrange later formalized these initial approaches into their celebrated necessary conditions for optimality, what we now call the Euler–Lagrange equations. For certain types of functionals, this approach reduces the optimization problem to solving a differential equation, i.e., the Euler–Lagrange equation, corresponding to the functional. Indeed, the reduction of an optimization problem to that of solving a differential equation can be

MSC2010: 49K05, 49K30, 49S05.

Keywords: brachistochrone problem, calculus of variations of one independent variable, eikonal equation, geometric optics.

directly applied to many classical optimization problems such as the isoperimetric problem [Blåsjö 2005], determining the shape of a minimal surface [Sagan 1969; Oprea 2000] and calculating the path of a geodesic on a surface [McCleary 2013]. Moreover, in classical mechanics the dynamics of a system can be derived using the Euler–Lagrange equations to extremize the so-called “action” of the system [Goldstein et al. 2014]. This approach to classical mechanics is equivalent to Newtonian mechanics but leads to deeper insights which are critical to our current mathematical understanding of quantum mechanics, general relativity, and other branches of physics.

While the Euler–Lagrange equations have been very successfully applied to many problems in engineering and physics, they do not provide the complete picture. In particular, as necessary conditions for optimality, their derivation implicitly assumes existence and smoothness of a minimum. In modern mathematics and applications these assumptions are naive. For instance, many problems in continuum mechanics have minimizers which lack enough regularity to be classical solutions to the Euler–Lagrange equations [Müller 1999]. The existence of these nonstandard solutions is not simply a mathematical curiosity but can be realized in practice as the blister and herringbone patterns in compressed thin sheets [Ortiz and Gioia 1994; Song et al. 2008], branched domain structures in ferromagnets [DeSimone et al. 2000], self-similar patterns in shape memory alloys [Bhattacharya 2003], the network of ridges in crumpled paper [Witten 2007], and even the fractal-like patterns in leaves and torn elastic sheets [Audoly and Boudaoud 2003; Sharon et al. 2007; Gemmer et al. 2016]. To understand such systems, local solutions of the Euler–Lagrange equations must be “patched together” along singularities in a manner that is consistent with the overall variational structure of the problem; see [Kohn 2007] for an introduction to this approach.

In this paper our focus is more modest. Namely, we study the problem of determining brachistochrone solutions for particles falling in an inverse-square gravitational field. This problem has been studied in [Parnovsky 1998; Tee 1999; Gemmer et al. 2011] using standard techniques from the calculus of variations. However, in these works they only considered “strong” solutions to the Euler–Lagrange equations, which limits the scope of the optimal paths considered. In particular, in [Parnovsky 1998; Tee 1999; Gemmer et al. 2011] it was shown that there is a “forbidden” region through which strong solutions to the Euler–Lagrange equations do not penetrate. In this paper, we show that by considering appropriate “weak” solutions constructed from strong solutions patched together at the singular origin of the gravitational field, the full space of optimal paths is more robust. In particular, these solutions enter the forbidden region and are characteristics for the Hamilton–Jacobi equation. This lends credence to the notion that our solutions are the natural extensions of the strong solutions that penetrate the forbidden region

and are optimal. Moreover, we also consider the inverse-square problem on an annular domain. Using variational inequalities, we show that our weak solutions are obtained in the limit as the inner radius of the annulus vanishes.

The paper is organized as follows. In [Section 2](#) we outline the general framework of brachistochrone problems, present the strong and weak versions of the Euler–Lagrange equations, and draw a connection to geometric optics using results from optimal control theory. In [Section 3](#) we restrict our focus to the case of the inverse-square gravitational field. We first briefly reproduce the results in [\[Parnovsky 1998; Tee 1999\]](#), namely that there exists a forbidden region through which strong solutions cannot penetrate. Next we present our construction of weak solutions that penetrate into this region. In [Section 4](#) we take a pragmatic approach and consider the problem on an annular domain that excises the singularity at the origin. In doing so, we prove that under the assumption that the strong solutions are global minimizers outside of the forbidden region, our weak solutions are time-optimal. We conclude with a discussion section.

2. Mathematical framework and governing equations

2.1. Mathematical framework. In this section we summarize the essential definitions and equations which we use to study brachistochrone problems in generic settings. First, let $V : \mathbb{R}^n \rightarrow \mathbb{R}$ be the potential for a gravitational field; i.e., V is a smooth function except possibly at isolated singularities. Suppose $A, B \in \mathbb{R}^n$ satisfy $V(A) > V(B)$ and there exists a smooth curve $\alpha : [0, 1] \rightarrow \mathbb{R}^n$ satisfying $\alpha(0) = A$, $\alpha(1) = B$ and $V(\alpha(s)) \leq V(A)$ for all $0 \leq s \leq 1$. Now, for a particle released in the gravitational field and constrained to fall along α , it follows that if friction is neglected, mechanical energy is conserved along the path

$$|\alpha'(s)|^2 \left(\frac{ds}{dt} \right)^2 + V(\alpha(s)) = V(A), \quad (1)$$

where t denotes time traveled on α and we have absorbed the standard factor of $1/2$ in the kinetic energy into the potential. The total time of flight to B can then be directly computed:

$$T[\alpha] = \int_0^1 \frac{|\alpha'(s)|}{\sqrt{V(A) - V(\alpha(s))}} ds. \quad (2)$$

This time of flight is still well defined if instead of smooth functions we consider *absolutely continuous functions* for which $V(\alpha) \leq V(A)$.¹ That is, we define the

¹The space of absolutely continuous functions from $[0, 1]$ into \mathbb{R}^n consists of all functions for which there exists a Lebesgue measurable function $\beta : [0, 1] \rightarrow \mathbb{R}^n$ satisfying $\alpha(s) = \alpha(0) + \int_0^s \beta(\bar{s}) d\bar{s}$ and is denoted by $AC([0, 1]; \mathbb{R}^n)$ [\[Leoni 2009\]](#). For $\alpha \in AC([0, 1]; \mathbb{R}^n)$ the (weak) notion of the first derivative is defined by $\alpha'(s) = \beta(s)$.

admissible set \mathcal{A} by

$$\mathcal{A} = \left\{ \alpha \in AC([0, 1]; \mathbb{R}^n) : \alpha(0) = A, \alpha(1) = B \text{ and } V(\alpha(s)) \leq V(A) \right\} \quad (3)$$

and define the functional $T : \mathcal{A} \rightarrow \mathbb{R}$ by (2). The generalized brachistochrone problem for the potential V is to find a curve $\alpha^* \in \mathcal{A}$ that minimizes the time of flight to B . We call such curves *brachistochrone solutions* for the potential V .

The contours, i.e., the equipotential curves, of V naturally partition \mathbb{R}^n into domains

$$U(A) = \{x \in \mathbb{R}^n : V(A) - V(x) \geq 0\}$$

that contain points that (possibly) can be reached by brachistochrone solutions. For example, for the uniform gravitational potential $V : \mathbb{R}^2 \rightarrow \mathbb{R}$, defined by $V(x, y) = -y$, a particle released at the point $A = (0, 0)$ can only reach points in the set $U(A) = \{(x, y) \in \mathbb{R}^2 : y \leq 0\}$. To completely solve the brachistochrone problem for this potential, one is naturally led to the question of finding all brachistochrone solutions that foliate $U(A)$.

2.2. Euler–Lagrange equations for brachistochrone problems. We now follow classical techniques presented in [Sagan 1969] to derive the Euler–Lagrange equations for (2). First, suppose $\inf_{\alpha \in \mathcal{A}} T[\alpha] < \infty$ and $\alpha^* \in \mathcal{A}$ satisfies $T[\alpha^*] = \inf_{\alpha \in \mathcal{A}} T[\alpha]$, i.e., α^* is a minimizer. Since $\alpha^* \in AC([0, 1]; \mathbb{R}^n)$ and $T[\alpha^*] < \infty$, the set of points in $[0, 1]$ for which $V(\alpha^*(s)) = A$ has Lebesgue measure zero. Consequently, if we further assume that $V(\alpha^*(s)) = V(A)$ only at $s = 0$ and possibly at $s = 1$ if the terminal point satisfies $V(B) = V(A)$, then for all $\eta \in C_0^\infty([0, 1]; \mathbb{R}^n)^2$ there exists $\bar{h} > 0$ such that $|h| < \bar{h}$ implies $\alpha^* + h\eta \in \mathcal{A}$. Define the function $f : [-\bar{h}, \bar{h}] \rightarrow \mathbb{R}$ by $f(x) = T[\alpha^* + h\eta]$. From the regularity assumptions on V and α^* , it follows that f is differentiable in h and consequently, since α^* minimizes T , it follows that $f'(0) = 0$. Therefore, we have the following necessary condition for optimality:

$$f'(0) = \int_0^1 \frac{\alpha^{*'}(s)}{|\alpha^{*'}(s)|\sqrt{V(A) - V(\alpha^*(s))}} \cdot \eta'(s) ds + \frac{1}{2} \int_0^1 \frac{|\alpha^{*'}(s)|}{(V(A) - V(\alpha^*(s)))^{3/2}} \nabla V(\alpha^*(s)) \cdot \eta ds, \quad (4)$$

which must be satisfied for all $\eta \in C_0^\infty([0, 1]; \mathbb{R}^n)$ [Evans 1998]. Equation (4) is known as the *weak formulation of the Euler–Lagrange equations for the brachistochrone problem*. If we further assume that the minimizing curve α^* is twice

² $C_0^\infty([0, 1]; \mathbb{R}^n)$ denotes the space of smooth functions from $[0, 1]$ into \mathbb{R}^n with compact support [Royden and Fitzpatrick 2010].

differentiable then (4) can be integrated by parts to yield

$$0 = \int_0^1 \left(\frac{1}{2} \frac{|\alpha^{*'}(s)|}{(V(A) - V(\alpha^*(s)))^{3/2}} \nabla V(\alpha^*(s)) - \frac{d}{ds} \left(\frac{\alpha^{*'}(s)}{|\alpha^{*'}(s)| \sqrt{V(A) - V(\alpha^*(s))}} \right) \right) \cdot \eta \, ds. \quad (5)$$

By the so-called “fundamental theorem of the calculus of variations”, since η was arbitrary the necessary condition satisfied by a twice differentiable curve α^* is the following differential equation [Sagan 1969]:

$$0 = \frac{1}{2} \frac{|\alpha^{*'}(s)|}{(V(A) - V(\alpha^*(s)))^{3/2}} \nabla V(\alpha^*(s)) - \frac{d}{ds} \left(\frac{\alpha^{*'}(s)}{|\alpha^{*'}(s)| \sqrt{V(A) - V(\alpha^*(s))}} \right). \quad (6)$$

Equation (6) is known as the *strong formulation of the Euler–Lagrange equations for the brachistochrone problem*.

Note, however, that in deriving the strong formulation of the Euler–Lagrange equations we made the additional assumption that α^* is twice differentiable. In many applications this assumption is too restrictive. For example, the functional $J : AC([-1, 1]; \mathbb{R}) \rightarrow \mathbb{R}$ defined by $J[y] = \int_{-1}^1 (1 - y'(s)^2)^2 \, ds$ with boundary conditions $y(-1) = y(1) = 1$ is minimized by $y(x) = |x|$. In this example the two strong solutions $y = x$ and $y = -x$ are joined together at $x = 0$. However simply gluing together two strong solutions does not guarantee that the resulting combination is a weak solution. If α^* is twice differentiable everywhere except at a point $c \in (0, 1)$ and satisfies (6) away from c , we can integrate (4) by parts to obtain the necessary condition

$$\lim_{s \rightarrow c^-} \left(\frac{\alpha^{*'}(s)}{|\alpha^{*'}(s)| \sqrt{V(A) - V(\alpha(s))}} \right) = \lim_{s \rightarrow c^+} \left(\frac{\alpha^{*'}(s)}{|\alpha^{*'}(s)| \sqrt{V(A) - V(\alpha(s))}} \right). \quad (7)$$

Equation (7) is commonly called the Weierstrass–Erdmann corner condition [Sagan 1969] and must be satisfied by piecewise smooth solutions of (6).

We now make some additional comments about the Weierstrass–Erdmann corner conditions which will be relevant to the discussion in later sections. First, away from a singularity in the potential V , i.e., if we assume that $(V(A) - V(c))^{-1/2} \neq 0$, (7) corresponds to continuity of the tangent vector $\alpha'(s)$ at c . Moreover, away from singularities, this condition physically corresponds to conservation of classical momentum at c . However, if $(V(A) - V(c))^{-1/2} = 0$, this necessary condition is trivially satisfied. That is, at a singularity in the gravitational field, a minimizer could violate conservation of momentum. This result should not be surprising since at a singularity $V(c) = \infty$, implying that the instantaneous speed, as well as the acceleration of the particle, is infinite. This fact will be critical in our later construction of weak brachistochrone solutions in an inverse-square gravitational field.

2.3. Connection with geometrical optics through control theory. While directly solving the Euler–Lagrange equations given by (6) will solve the brachistochrone problem, there is another approach, originally taken by Johann Bernoulli. Namely, Bernoulli realized that the brachistochrone problem is equivalent to finding the path traced out by a ray of light in a medium with index of refraction $n(\mathbf{x}) = (V(A) - V(\mathbf{x}))^{-1/2}$. His solution method was prescient in that it applied Snell’s law of refraction to what would now be called a finite element approximation to the problem with a piecewise linear basis [Erlichson 1999; Sussmann and Willems 1997]. The connection to geometrical optics was later exploited by Hamilton and finalized by Jacobi to derive what we now call the Hamilton–Jacobi equations for a variational problem [Broer 2014; Sussmann and Willems 1997; Nakane and Fraser 2002]. Specifically, the Hamilton–Jacobi equation is a quasilinear partial differential equation whose characteristic equations are precisely the Euler–Lagrange equations for the system [Evans 1998]. In particular, the Hamilton–Jacobi equation governs the dynamics of wave-fronts propagating in a medium with index of refraction $n(\mathbf{x})$ and the Euler–Lagrange equations are the evolution equations for the normals to the wave-fronts.

We will now show how the geometric optics interpretation of the brachistochrone problem can be directly derived using modern optimal control theory. To reinterpret the brachistochrone problem as a control problem we follow [Sussmann and Willems 1997] and first define the set of admissible controls by

$$\mathcal{U} = \{\mathbf{u} : [0, \mathbb{R}) \rightarrow \mathbb{R}^n : \mathbf{u} \text{ is piecewise smooth and } |\mathbf{u}| = 1\}, \quad (8)$$

and to satisfy (1) we constrain the dynamics of the system by

$$\dot{\alpha} = \sqrt{V(A) - V(\mathbf{x})} \mathbf{u}. \quad (9)$$

We define the *trajectory of a control* to be the curve α defined by (9) and also define $\mathcal{T}_B : \mathcal{U} \rightarrow \mathbb{R} \cup \{+\infty\}$ to be the first time a trajectory corresponding to a control \mathbf{u} reaches the point B . The optimal control problem corresponding to the brachistochrone problem is to find $\mathbf{u}^* \in \mathcal{U}$ that steers a trajectory $\alpha(t)$ to a point $B \in U(A)$ in the minimal amount of time. That is, find $\mathbf{u}^* \in \mathcal{U}$ such that $T_B[\mathbf{u}^*] = \inf_{\mathbf{u} \in \mathcal{U}} \mathcal{T}_B[\mathbf{u}]$. Clearly, this optimal control problem is equivalent to our previous formulation of the brachistochrone problem and $\inf_{\mathbf{u} \in \mathcal{U}} \mathcal{T}_B[\mathbf{u}] = \inf_{\alpha \in \mathcal{A}} T[\alpha]$.

One technique for solving such an optimal control problem is to apply Bellman’s technique of dynamic programming [Bertsekas 1995]. Namely, if we define the *value function* $\mathcal{V} : U(A) \rightarrow \mathbb{R}$ by

$$\mathcal{V}(\mathbf{x}) = \inf_{\mathbf{u} \in \mathcal{U}} \mathcal{T}_x[\mathbf{u}] \quad (10)$$

then the dynamic programming principle states that for $\Delta t > 0$ sufficiently small

$$\mathcal{V}(\mathbf{x}) = \min_{\substack{\mathbf{u} \in \mathcal{U} \\ 0 < s < \Delta t}} \{\mathcal{V}(\bar{\alpha}(\Delta t)) + \Delta t\}, \quad (11)$$

where $\bar{\alpha}$ corresponds to the *time-reversed* solution of (9) with initial condition $\bar{\alpha}(0) = \mathbf{x}$ and control \mathbf{u} . If we assume that \mathcal{V} is smooth, we can formally Taylor expand:

$$\mathcal{V}(\mathbf{x}) = \min_{|\mathbf{u}(0)|=1} \left\{ \mathcal{V}(\mathbf{x}) + \nabla \mathcal{V}(\mathbf{x}) \sqrt{V(A) - V(\mathbf{x})} \mathbf{u}(0) \Delta t + \Delta t + \mathcal{O}(\Delta t^2) \right\}.$$

Consequently, taking the limit as $\Delta t \rightarrow 0$, we obtain

$$-1 = \min_{|\mathbf{u}(0)|=1} \nabla \mathcal{V}(\mathbf{x}) \sqrt{V(A) - V(\mathbf{x})} \mathbf{u}(0).$$

Finally, this minimum is obtained by $\mathbf{u}(0) = -\nabla \mathcal{V}(\mathbf{x})/|\nabla \mathcal{V}(\mathbf{x})|$ and hence we can conclude that the value function \mathcal{V} satisfies the partial differential equation

$$|\nabla \mathcal{V}|^2 = \frac{1}{V(A) - V(\mathbf{x})} = n^2(\mathbf{x}). \tag{12}$$

In geometrical optics, (12) is an eikonal equation for a medium with index of refraction $n(\mathbf{x})$. That is, the level sets of solutions to (12) correspond to wave fronts for light traveling through the medium and the light rays correspond to curves that are everywhere tangent to the normals of the level sets of \mathcal{V} . Consequently, if we let $\beta(s)$ be an arc-length parametrization of such a light ray, it follows that

$$\nabla \mathcal{V}(\beta(s)) = n(\beta(s)) \frac{d\beta}{ds}. \tag{13}$$

Differentiating with respect to ds and switching the order of differentiation,

$$\nabla \left(\nabla \mathcal{V}(\beta(s)) \cdot \frac{d\beta}{ds} \right) = \frac{d}{ds} \left(n(\beta(s)) \frac{d\beta}{ds} \right).$$

Therefore, by (12) and (13), the governing equation for the rays is

$$\nabla n(\beta) = \frac{d}{ds} \left(n(\beta(s)) \frac{d\beta}{ds} \right). \tag{14}$$

Finally, it follows immediately that (14) is simply a version of (6) that is parametrized by arc-length. That is, to solve the brachistochrone problem we could, in principle, solve the eikonal equation (12) and use (13) to reconstruct the brachistochrone solution. More importantly, we could solve the brachistochrone problem directly by solving the Euler–Lagrange equations (6) and compute the time of flight along these solution curves to compute the solution to the eikonal equation (12).

3. Brachistochrone problem in an inverse-square gravitational field

3.1. Framework. Consider two points $A, B \in \mathbb{R}^2$ with $|B| \leq |A|$. For an inverse-square field, the potential $V : \mathbb{R}^2 \rightarrow \mathbb{R}$ is defined by $V(x) = -|x|^{-2}$. The inverse-square brachistochrone problem is to construct a curve connecting A and B such

that a particle traversing the curve from A to B under the influence a gravitational field centered at the origin with potential V has the least time of flight. In this case the admissible set \mathcal{A}_0 is defined by

$$\mathcal{A}_0 = \{ \alpha \in AC([0, 1]; \mathbb{R}^2) : \alpha(0) = A, \alpha(1) = B \text{ and } \forall t \in [0, 1], |\alpha(t)| \leq |A| \} \quad (15)$$

and the time of flight $T : \mathcal{A}_0 \rightarrow \mathbb{R}^+$ is given by

$$T[\alpha] = \int_0^1 \frac{|\alpha'(s)|}{\sqrt{|\alpha(s)|^{-2} - |A|^{-2}}} ds. \quad (16)$$

Again, this functional arises from classical conservation of mechanical energy and the constraint $|\alpha(s)| \leq |A|$ — a necessary condition for this functional to be well defined — is equivalent to the condition that the particle cannot gain mechanical energy.

To study minimizers of (16) it is natural to work in a polar-coordinate representation of the form

$$\alpha(s) = (r(s) \cos(\theta(s)), r(s) \sin(\theta(s))), \quad (17)$$

where $r : [0, 1] \rightarrow [0, |A|]$ and $\theta : [0, 1] \rightarrow [-\pi, \pi]$ are (weakly) differentiable functions satisfying $r(0) = |A|$, $r(1) = |B|$, $\theta(0) = \theta_0$, $\theta(1) = \theta_f$, with θ_0, θ_f the angular coordinates of A, B respectively; see Figure 1 (left). By rotational symmetry and radial invariance we can assume without loss of generality that $A = (1, 0)$; see Figure 1 (right). In this representation, (16) becomes

$$T[r, \theta] = \int_0^1 \sqrt{\frac{r'(s)^2 + r(s)^2 \theta'(s)^2}{r(s)^{-1} - 1}} ds = \int_0^1 L_2(r(s), r'(s), \theta'(s)) ds, \quad (18)$$

where $L_2 : \mathbb{R}^3 \rightarrow \mathbb{R}$ denotes the Lagrangian for this functional. To reduce encumbering notation we write $(r(s), \theta(s)) \in \mathcal{A}_0$ as a proxy for the statement that there exists $\alpha \in \mathcal{A}_0$ with corresponding radial and angular components $r(s)$ and $\theta(s)$ respectively.

We now deduce geometric properties of minimizers using the structure of the Lagrangian. We first show that if $(r^*, \theta^*) \in \mathcal{A}_0$ minimizes T then θ^* must be a monotone function. This property prevents a minimizer from “turning back” to its starting point. The idea of the proof is to construct for all $(r, \theta) \in \mathcal{A}_0$ a modified curve $(r, \bar{\theta}) \in \mathcal{A}$ with $\bar{\theta}$ monotone in s and show $T[r, \bar{\theta}] \leq T[r, \theta]$.

Proposition 1. *If $(r^*(s), \theta^*(s)) \in \mathcal{A}_0$ minimizes T then θ^* is monotone in s .*

Proof. Let $(r(s), \theta(s)) \in \mathcal{A}_0$ terminate at the point $(r_f \cos \theta_f, r_f \sin \theta_f)$ and assume $\theta_f \geq 0$. Define $\bar{\theta} : [0, 1] \rightarrow [0, 2\pi]$ by $\bar{\theta}(s) = \min\{\theta_f, \sup\{\theta(t) : 0 \leq t \leq s\}\}$. From the absolute continuity of θ , it follows that $\bar{\theta}$ is absolutely continuous, monotone

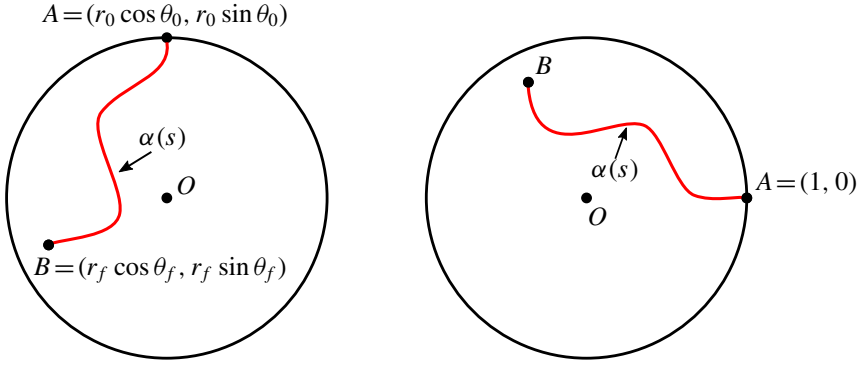


Figure 1. Left: Plot of a curve $\alpha : [0, 1] \rightarrow \mathbb{R}^2$ connecting $A = (r_0 \cos \theta_0, r_0 \sin \theta_0)$ to $B = (r_f \cos \theta_f, r_f \sin \theta_f)$ in an inverse-square gravitational field centered at the origin O . The circle of radius r_0 is an equipotential for the inverse-square gravitational field. For a particle falling along this curve, conservation of mechanical energy requires that $|\alpha(s)| \leq r_0$. Right: By rotational and radial scale invariance of this problem, we can assume without loss of generality that $A = (1, 0)$.

increasing and satisfies $\bar{\theta}(1) = \theta_f$. Moreover, there exists a closed set I on which $\bar{\theta} = \theta$ and an open set $\bar{I} = [0, 1] \setminus I$ on which $d\bar{\theta}/ds = 0$. Therefore,

$$\begin{aligned} T[r, \bar{\theta}] &= \int_I \sqrt{\frac{r'(s)^2 + r(s)^2 \theta'(s)^2}{r(s)^{-1} - 1}} ds + \int_{\bar{I}} \sqrt{\frac{r'(s)^2}{r(s)^{-1} - 1}} ds \\ &\leq \int_I \sqrt{\frac{r'(s)^2 + r(s)^2 \theta'(s)^2}{r(s)^{-1} - 1}} ds + \int_{\bar{I}} \sqrt{\frac{r'(s)^2 + r(s)^2 \theta'(s)^2}{r(s)^{-1} - 1}} ds = T[r, \theta], \end{aligned}$$

with equality if and only if θ is monotone increasing. Thus, if $(r^*(s), \theta^*(s)) \in \mathcal{A}_0$ minimizes T then θ^* is monotone increasing in s . A similar argument proves that θ^* must be monotone decreasing if $\theta_f < 0$. □

We now prove that without loss of generality we can assume minimizers are symmetric about the angle $\theta_f/2$. Specifically, if in polar coordinates $(r^*(s), \theta^*(s)) \in \mathcal{A}_0$ minimizes T and terminates at the final point $(r_f = 1, \theta_f)$ then the image of $(r(s), \theta(s))$ is symmetric about the line $\theta = \theta_f/2$. Similar to the previous proof, the idea is to modify a curve $\alpha \in \mathcal{A}_0$ by constructing symmetric versions and comparing the times of flight.

Proposition 2. *If $(r^*(s), \theta^*(s)) \in \mathcal{A}_0$ minimizes T with terminal point $(r(1), \theta(1)) = (1, \theta_f)$ then there exists a version of $(r^*(s), \theta^*(s))$ in \mathbb{R}^2 that is symmetric about the line $\theta = \theta_f/2$ that also minimizes T .*

Proof. Let $(r(s), \theta(s)) \in \mathcal{A}_0$ and $t(s)$ be a reparameterization in which $\theta(1/2) = \theta_f/2$ and if $t > 1/2$ then $\theta(t) > \theta_f/2$. Define the two possible reflections of $(r(t), \theta(t))$ about the line $\theta = \theta_f/2$ by

$$r_1(t) = \begin{cases} r(t), & 0 \leq t \leq \frac{1}{2}, \\ r(1-t), & \frac{1}{2} < t \leq 1, \end{cases} \quad \text{and} \quad \theta_1(t) = \begin{cases} \theta(t), & 0 \leq t \leq \frac{1}{2}, \\ \theta_f - \theta(1-t), & \frac{1}{2} < t \leq 1, \end{cases}$$

$$r_2(t) = \begin{cases} r(1-t), & 0 \leq t \leq \frac{1}{2}, \\ r(t), & \frac{1}{2} < t \leq 1, \end{cases} \quad \text{and} \quad \theta_2(t) = \begin{cases} \theta(1-t) - \theta_f, & 0 \leq t \leq \frac{1}{2}, \\ \theta(t), & \frac{1}{2} < t \leq 1. \end{cases}$$

By construction, the images of the curves $(r_1(t), \theta_1(t))$ and $(r_2(t), \theta_2(t))$ in \mathbb{R}^2 are symmetric about the line $\theta = \theta_f/2$. It follows from symmetry that

$$T[r_1, \theta_1] = 2 \int_0^{1/2} \sqrt{\frac{r'(s)^2 + r(s)^2 \theta'(s)^2}{r(s)^{-1} - 1}} ds,$$

$$T[r_2, \theta_2] = 2 \int_{1/2}^1 \sqrt{\frac{r'(s)^2 + r(s)^2 \theta'(s)^2}{r(s)^{-1} - 1}} ds.$$

Therefore, $T[r_1, \theta_1] + T[r_2, \theta_2] = 2T[r, \theta]$ from which it follows that

$$\min\{T[r_1, \theta_1], T[r_2, \theta_2]\} \leq T[r, \theta].$$

Thus if $(r^*(s), \theta^*(s)) \in \mathcal{A}_0$ minimizes T then either $(r_1(s), \theta_1(s))$ or $(r_2(s), \theta_2(s))$ must also minimize T . □

3.2. Strong solutions to Euler–Lagrange equations. In this subsection we review the construction of smooth minimizers to T that was originally presented in [Parnovsky 1998; Tee 1999]. The classic method for finding time-minimizing curves is to derive the Euler–Lagrange equations for T and solve the resulting boundary value problem. Specifically, if we assume there exists a twice differentiable curve $\alpha^*(s) \in \mathcal{A}_0$ with angular component $\theta^*(s)$ and radial component $r^*(s)$ that (locally) minimizes T then the resulting boundary value problem is

$$\begin{cases} \left(\frac{\partial L}{\partial r} - \frac{d}{ds} \frac{\partial L}{\partial r'} \right) \Big|_{(r^*(s), \theta^*(s))} = 0, \\ \frac{d}{ds} \frac{\partial L}{\partial \theta'} \Big|_{(r^*(s), \theta^*(s))} = 0, \\ r^*(0) = 1, r^*(1) = |B|, \theta^*(0) = 0, \theta(1) = \theta_f. \end{cases} \tag{19}$$

If we make the assumption that θ^* is a function of r^* , i.e., we assume the ansatz $r^*(s) = (|B| - 1)s + 1$, then (19) reduces to the differential equation

$$\frac{d}{dt} \frac{\partial L}{\partial \theta'} = 0. \tag{20}$$

Formally, (20) can be integrated to yield a separable differential equation with solution

$$\theta^*(r^*) = \pm \int_1^{r^*} \sqrt{\frac{2(1/u - 1)D}{u^4 - u^2(2(1/u - 1))D}} du, \tag{21}$$

where $D > 0$ is a constant of integration which can be determined from the boundary conditions. The assumption that θ^* is globally a function of r^* is valid if $(d\theta^*/dr^*)^{-1} \neq 0$ for all $r^* \in (0, 1)$. It follows from (21) that for fixed $D > 0$ this condition is equivalent to the nonexistence of solutions to the equation $r^3 + 2Dr - 2D = 0$ for $r \in (0, 1]$. The following proposition makes this statement precise and identifies the critical radius r_c in terms of the integration constant D .

Proposition 3. *For fixed $D > 0$, there exists a unique $r_c(D) \in [0, 1]$ such that $\theta^*(r^*)$ defined by (21) satisfies*

$$\lim_{r \rightarrow r_c(D)^+} \frac{d\theta^*}{dr^*} \Big|_r = \infty.$$

Moreover, the mapping $D \rightarrow r_c(D)$ is a bijection from $(0, \infty)$ into $(0, 1)$.

Proof. Fix $D > 0$ and define $g : (0, 1) \rightarrow \mathbb{R}$ by $g(r) = r^3 + 2Dr - 2D$. Since $g(0) = -2D$, $g(1) = 1$, and $g'(r) > 0$, by the intermediate value theorem there exists unique $r_c(D) \in (0, 1)$ such that $g(r_c(D)) = 0$. Consequently, it follows from (21) that

$$\lim_{r \rightarrow r_c(D)^+} \frac{\partial \theta^*}{\partial r^*} \Big|_r = \infty.$$

The bijection is proved by noting that the inverse mapping from $r_c(D)$ to D given by $D(r_c) = (r_c^3/2)(1 - r_c)$ satisfies $\lim_{r_c \rightarrow 0^+} D(r_c) = 0$, $\lim_{r_c \rightarrow 1^-} D(r_c) = \infty$ and is monotone increasing in r_c . □

To extend smooth solutions beyond the point where θ^* is no longer a function of r^* it follows from Proposition 2 that it is necessary to reflect the solutions across the line $\theta = \theta_f/2$. Specifically, for $D \in (0, \infty)$ if we define $r_c(D)$ as in Proposition 3 then we obtain the following family of solutions expressed in parametric form $\alpha(s) = (r_D^S(s) \cos(\theta_D^S(s)), r_D^S(s) \sin(\theta_D^S(s)))$ with

$$r_D^S(s) = \begin{cases} 2(r_c(D) - 1)s + 1, & 0 \leq s \leq \frac{1}{2}, \\ 2(1 - r_c(D))(s - 1) + 1, & \frac{1}{2} < s \leq 1, \end{cases} \tag{22}$$

$$\theta_D^S(s) = \begin{cases} \pm \int_1^{r_D^S(s)} \sqrt{\frac{2(1-u)D}{u^5 - 2u^2D(1-u)}} du, & 0 \leq s \leq \frac{1}{2}, \\ \mp \int_{r_c(D)}^{r_D^S(s)} \sqrt{\frac{2(1-u)D}{u^5 - 2u^2D(1-u)}} du \pm \theta_D^S\left(\frac{1}{2}\right), & \frac{1}{2} \leq s \leq 1, \end{cases} \tag{23}$$

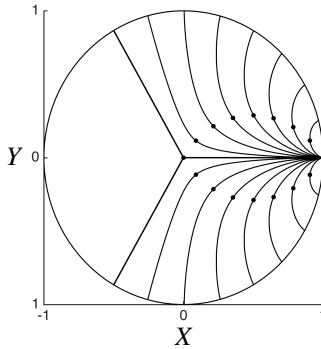


Figure 2. Plot of 16 smooth strong solution curves $\alpha(s)$ defined by (22) and (23) with the final angular coordinate $\theta_D^S(1)$ uniformly spaced from $-\pi/3$ to $\pi/3$. The value of D was found by the bisection method, i.e., the shooting method, applied to (23). The points indicate the critical radius $r_c(D)$ where $d\theta_D^S/dr_D^S = \pm\infty$ and the curve begins receding away from the origin.

where we are using the superscript “S” to denote that these are strong solutions to the Euler–Lagrange equations. Note, that while the individual functions $r_D^S(s)$ and $\theta_D^S(s)$ are not smooth, the curve α itself is a smooth function from $[0, 1]$ into \mathbb{R}^2 .

Interestingly, as D ranges over values in $(0, \infty)$ the curves defined by (22) and (23) do not foliate the unit disk $x^2 + y^2 \leq 1$; see Figure 2. Indeed, if we define the sector S by

$$S = \{\theta : -\pi \leq \theta < -2\pi/3\} \cup \{\theta : 2\pi/3 < \theta < \pi\}, \tag{24}$$

it was shown in [Tee 1999; Gemmer et al. 2011] that these curves do not enter S . This is made precise by the following proposition whose proof we adapt from [Gemmer et al. 2011].

Proposition 4. *For all $s \in [0, 1]$ and $D \in (0, \infty)$ the curves $\alpha(s)$ with radial and angular components $r_D^S(s)$ and $\theta_D^S(s)$ defined by (22) and (23) satisfy $\theta_D^S(s) \notin S$.*

Proof. For $D > 0$ let $\alpha(s) = (r_D^S(s) \cos(\theta_D^S(s)), r_D^S(s) \sin(\theta_D^S(s)))$ be defined by (22) and (23) with the “–” branch. Differentiating,

$$\frac{d\theta_D^S}{ds} = \frac{d\theta_D^S}{dr_D^S} \frac{dr_D^S}{ds} = 2r_c(D) \sqrt{\frac{2(1-r_D^S)D}{(r_D^S)^5 - 2(r_D^S)^2 D(1-r_D^S)}} > 0$$

with equality only at $r_D^S = 1$. Hence, $d\theta_D^S/ds$ is monotone increasing in s with the maximum angular coordinate $\bar{\theta}(D)$ satisfying

$$\bar{\theta}(D) = \max_{0 \leq s \leq 1} \theta_D^S(s) = 2 \int_{r_c(D)}^1 \sqrt{\frac{2(1-u)D}{u^5 - 2u^2 D(1-u)}} du.$$

Since $\lim_{D \rightarrow \infty} r_c(D) = 1$, it follows that $\lim_{D \rightarrow \infty} \bar{\theta}(D) = 0$. Now, from uniqueness of solutions to (20) we can deduce that $\bar{\theta}(D)$ must be monotone decreasing in D and hence has a limit as $D \rightarrow 0$. By making the change of variables $x = r_c(D)/u^{3/2}$, we obtain

$$\begin{aligned} \frac{1}{2} \lim_{D \rightarrow 0} \bar{\theta}(D) &= \lim_{D \rightarrow 0} \frac{2}{3} \int_{r_c(D)}^1 \sqrt{\frac{1 - r_c(D)x^{-2/3}}{(1 - r_c(D)) - (1 - r_c(D)x^{-2/3})x^2}} dx \\ &= \lim_{D \rightarrow 0} \frac{2}{3} \int_0^1 \sqrt{\frac{1}{(1 - r_c(D))/(1 - r_c(D)x^{-2/3}) - x^2}} \mathbb{I}\{x > r_c(D)^{3/2}\} dx, \end{aligned}$$

where \mathbb{I} denotes the standard indicator function. Now, observing that the integrand of the above equation forms a sequence of functions bounded by $(1 - x^2)^{-1/2}$, it follows from Lebesgue’s dominated convergence theorem that

$$\lim_{D \rightarrow 0} \bar{\theta}(D) = \int_0^1 \frac{4}{3} \sqrt{\frac{1}{1 - x^2}} dx = \frac{4}{3} (\arcsin(1) - \arcsin(0)) = \frac{2\pi}{3}.$$

The exact same arguments hold if we consider the “+” branch in (22) and (23) except the limiting angle is $-\pi/3$. Consequently we can conclude for all $s \in [0, 1]$ and $D \in (0, \infty)$ that $\theta_D^S(s)$ given by (23) satisfies

$$-\frac{2\pi}{3} \leq \theta_D^S(s) \leq \frac{2\pi}{3}. \quad \square$$

The following proposition immediately follows from Propositions 3 and 4.

Proposition 5. *For all $\theta_f \in (0, 2\pi/3)$ there exists $D \in (0, \infty)$ such that the solution curve with angular and radial coordinates $(\theta_D^S(s), r_D^S(s))$ as defined by (22) and (23) satisfies $\theta_D^S(0) = 0$, and $\theta_D^S(1) = \theta_f$. Moreover, the mapping $\theta_f \rightarrow D$ is a bijection.*

Remark. It follows from Propositions 3 and 4 that θ_f , r_c and D characterize a unique solution curve of the form defined by (22) and (23).

3.3. Weak solutions to the Euler–Lagrange equations. One family of weak solutions to (16) is given by the parametrization

$$r^W(s) = \begin{cases} 1 - 2s, & 0 \leq s \leq \frac{1}{2}, \\ 2s - 1, & \frac{1}{2} < s \leq 1, \end{cases} \tag{25}$$

$$\theta_{\theta_f}^W(s) = \begin{cases} 0, & 0 \leq s \leq \frac{1}{2}, \\ \theta_f, & \frac{1}{2} \leq s \leq 1, \end{cases} \tag{26}$$

where the superscript “W” is used to denote that these are weak solutions to the Euler–Lagrange equations. This parametrization indeed satisfies the corner

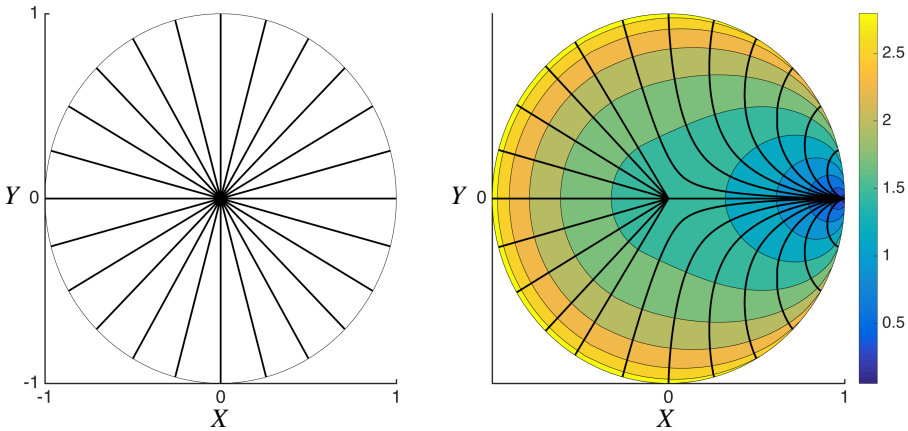


Figure 3. Left: Plot of weak solution curves defined by (25) and (26) with final angular coordinate θ_f spaced evenly from $-\pi$ to π . Right: Foliation of the unit disk by weak solution curves in S and classic solutions outside of S . Beneath the solution curves is a contour plot of the time of flight calculated along the solution curves. The contours correspond to level sets of the value \mathcal{V} satisfying the eikonal equation defined by (12).

condition given by (7):

$$\begin{aligned} & \lim_{s \rightarrow c^-} \left(\frac{\alpha^{*'}(s)}{|\alpha^{*'}(s)|\sqrt{V(A)-V(\alpha(s))}} \right) - \lim_{s \rightarrow c^+} \left(\frac{\alpha^{*'}(s)}{|\alpha^{*'}(s)|\sqrt{V(A)-V(\alpha(s))}} \right) \\ &= (1, 0) \lim_{s \rightarrow 1/2^+} \left(\sqrt{\frac{r^W(s)}{r^W(s)-1}} \right) + (\cos\theta_f, \sin\theta_f) \lim_{s \rightarrow 1/2^-} \left(\sqrt{\frac{r^W(s)}{r^W(s)-1}} \right) = (0, 0). \end{aligned}$$

It is important to note that as it is defined, $\theta_{\theta_f}^W(s)$ is not weakly differentiable. Specifically, $\theta_{\theta_f}^W(s)$ is only differentiable in the distributional sense with a derivative given by a delta mass centered at $s = 1/2$. However, this is only an artifact of the $r = 0$ coordinate singularity for polar coordinates and the curve $\alpha^W(s)$ itself is weakly differentiable. Moreover, for $s < 1/2$ this curve is simply the solution curve given by (22) and (23) with $D = 0$ and the weak solution is constructed by joining appropriately rotated copies of this strong solution at the origin.

The family of solutions to the Euler–Lagrange equations defined by (25) and (26) completely foliate the unit disk; see Figure 3 (left). Hence these solution curves are natural candidates for time minimizers that enter the sector S . In Figure 3 (right) we plot the unit disk foliated by a combination of strong and weak solutions to the Euler–Lagrange equations. More specifically, for a given θ_f we use (22) and (23) or (25) and (26) depending on whether $|\theta_f| > 2\pi/3$. The contour beneath the curves in corresponds to the time of flight computed along the solution curves and

confirms our intuition that the classic solutions have shorter time of flight outside of S . Notice that the contours in [Figure 3](#) (right) are smooth and intersect the strong and weak solution curves orthogonally as expected from [\(13\)](#). Moreover, the value function \mathcal{V} defined in [Section 2](#) is a solution to the eikonal equation defined by [\(12\)](#).

4. Constrained inverse-square brachistochrone problem

4.1. Variational inequality. In the previous section we solved the inverse-square brachistochrone problem using a combination of weak and strong extremizers. However, the solutions are impractical in that, as a consequence of the singular gravitational field, a particle following along an extremizer will experience infinite acceleration at the origin. To alleviate this problem we now consider a modified version of the inverse-square brachistochrone problem that restricts the radial coordinate to remain bounded away from the origin. Specifically, for $\epsilon > 0$ we define the annulus $\mathcal{O}_\epsilon = \{(x, y) \in \mathbb{R}^2 : \sqrt{x^2 + y^2} \geq \epsilon\}$ and consider the problem of minimizing T over the admissible set $\mathcal{A}_\epsilon \subset \mathcal{A}_0$ defined by

$$\mathcal{A}_\epsilon = \{(r(s), \theta(s)) \in \mathcal{A}_0 : (r(s) \cos(\theta(s)), r(s) \sin(\theta(s))) \in \mathcal{O}_\epsilon \text{ for } s \in [0, 1]\}. \quad (27)$$

This formulation of the problem is equivalent to an ‘‘obstacle problem’’ with the obstacle being the circle of radius ϵ centered at the origin.

To derive necessary conditions satisfied by minimizers of T over \mathcal{A}_ϵ we follow [\[Evans 1998, Chapter 8, Section 4\]](#) and derive a variational inequality that plays the role of the Euler–Lagrange equations. First, suppose $\alpha^*(s) \in \mathcal{A}_\epsilon$ is the global minimizer of T over \mathcal{A}_ϵ with radial and angular components $r^*(s)$ and $\theta^*(s)$ respectively. Letting $\beta(s) \in \mathcal{A}_\epsilon$ with radial and angular components $q(s)$ and $\theta^*(s)$ respectively, it follows from the convexity of \mathcal{A}_ϵ that for all $\lambda \in [0, 1]$ the curve $\gamma(s)$ with radial component $r^*(s) + \lambda(q(s) - r^*(s))$ and angular component $\theta^*(s)$ also satisfies $\gamma(s) \in \mathcal{A}_\epsilon$. Consequently

$$T[r^*(s) + \lambda(q(s) - r^*(s)), \theta^*(s)] - T[r^*(s), \theta^*(s)] \geq 0 \quad (28)$$

and thus taking the limit $\lambda \rightarrow 0$ we obtain the following necessary condition satisfied by a minimizer:

$$\int_0^1 \left((q(s) - r^*(s)) \frac{\partial L}{\partial r} \Big|_{r^*(s), \theta^*(s)} + (q'(s) - r^{*\prime}(s)) \frac{\partial L}{\partial r'} \Big|_{r^*(s), \theta^*(s)} \right) ds \geq 0. \quad (29)$$

Since we can perturb $\theta^*(s)$ by any smooth function ξ compactly supported on $[0, 1]$, we again obtain the weak Euler–Lagrange equation

$$\int_0^1 \xi'(s) \frac{\partial L}{\partial \theta'} \Big|_{r^*(s), \theta^*(s)} ds = 0. \quad (30)$$

We now illustrate how (29) and (30) can be used to derive further necessary conditions satisfied by a minimizer $(r^*(s), \theta^*(s)) \in \mathcal{A}_\epsilon$. Suppose $(r^*(s), \theta^*(s)) \in \mathcal{A}_\epsilon$ minimizes T over \mathcal{A}_ϵ and define the sets

$$U = (r^*)^{-1}\{\epsilon\}, \tag{31}$$

$$U^c = [0, 1] \setminus U. \tag{32}$$

Since $r^*(s)$ is continuous, U is a closed subset of $[0, 1]$. On U it follows that (29) is automatically satisfied since

$$\begin{aligned} \int_U \left((q(s) - r^*(s)) \frac{\partial L}{\partial r} \Big|_{r^*(s), \theta^*(s)} + (q'(s) - r'^*(s)) \frac{\partial L}{\partial r'} \Big|_{r^*(s), \theta^*(s)} \right) ds \\ = \int_U (q(s) - \epsilon) \frac{|\theta^{*'}(s)|}{1 - \epsilon} \frac{3 - 2\epsilon}{2} ds \geq 0. \end{aligned}$$

On U^c consider the perturbation $q(s) = \tau v(s) + r^*(s)$, where v is any smooth function compactly supported on V and $\tau \in \mathbb{R}$ is small enough in magnitude that $q(s) \in \mathcal{A}_\epsilon$. Substituting into (29) yields

$$\tau \int_{U^c} \left(v(s) \frac{\partial L}{\partial r} \Big|_{r^*(s), \theta^*(s)} + v'(s) \frac{\partial L}{\partial r'} \Big|_{r^*(s), \theta^*(s)} \right) ds \geq 0. \tag{33}$$

Since τ is of arbitrary sign, the above inequality is actually an equality. That is, for $s \in U^c$ we recover the weak Euler–Lagrange equations for $r^*(s)$.

Remark. Taken together, the above necessary conditions imply that potential minimizers of T over \mathcal{A}_ϵ consist of the family of curves satisfying the Euler–Lagrange equations away from the constraint. That is, potential minimizers consist of piecewise smooth curves satisfying (22) and (23), joined with circular arcs of radius ϵ .

4.2. Piecewise smooth minimum. As in the case with no constraint, i.e., $\epsilon = 0$, we now foliate \mathcal{O}_ϵ by curves that minimize the time of flight. By symmetry we only foliate the upper half-annulus $\mathcal{O}_\epsilon^+ = \{(x, y) \in \mathcal{O}_\epsilon : y \geq 0\}$. To construct the foliation we examine the behavior of potential minimizers with terminal coordinates (r_t, θ_f) satisfying $(r_f, \theta_f) \in \partial\mathcal{O}_\epsilon^+$ (the boundary of \mathcal{O}_ϵ^+) which can be naturally divided into four regions:

$$\begin{aligned} R_1 &= \{(r, \theta) \in \partial\mathcal{O}_\epsilon^+ : \theta = 0\}, & R_2 &= \{(r, \theta) \in \partial\mathcal{O}_\epsilon^+ : r = 1\}, \\ R_3 &= \{(r, \theta) \in \partial\mathcal{O}_\epsilon^+ : \theta = \pi\}, & R_4 &= \{(r, \theta) \in \partial\mathcal{O}_\epsilon^+ : r = \epsilon\}. \end{aligned}$$

Each of these regions is considered as separate cases below.

4.2.1. Minimizers terminating on R_1 . It follows from (22) and (23) that if $D = 0$, the strong solution to the Euler–Lagrange equation is a straight line connecting $(1, 0)$ to the origin. In particular this implies that if $(r_f, \theta_f) \in R_1$ then straight lines are the natural candidate minimizers.

4.3. Minimizers terminating on R_2 . Suppose $(r_f, \theta_f) \in R_2$. For θ_f sufficiently small we expect the minimizers to consist of the smooth strong solution curves defined by (22) and (23). However, if $\theta_f > \pi/3$, the strong solutions to the Euler–Lagrange equations will necessarily intersect the obstacle. Note that from the convexity of the strong solutions there exists a unique critical angle $\theta_c^\epsilon \in (0, \pi/3)$ in which the strong solutions intersect the obstacle tangentially. Specifically, θ_c^ϵ is defined by

$$\left(r_{D(\epsilon)}^S(1/2), \theta_{D(\epsilon)}^S\left(\frac{1}{2}\right) \right) = (\epsilon, \theta_c^\epsilon) \quad \text{and} \quad \left. \frac{dr_{D(\epsilon)}^S}{ds} \right|_{1/2} = 0. \tag{34}$$

The critical angle θ_c^ϵ serves as a boundary in the sense that if the final angular coordinate θ_f satisfies $\theta_f/2 > \theta_c^\epsilon$ then it is necessary to consider piecewise-defined curves as candidate minimizers. This is made precise by the following proposition.

Proposition 6. *Suppose that the smooth solution curves given by (22) and (23) are global minimizers of T over \mathcal{A}_0 . For $\epsilon > 0$, if $\theta_f/2 < \theta_c^\epsilon$ then there exists a $D \geq D(\epsilon) > 0$ such that $(r_D^S(s), \theta_D^S(s)) \in \mathcal{A}_\epsilon$ minimizes T over curves in \mathcal{A}_ϵ terminating at the angular coordinate θ_f .*

Proof. Let $\theta_f \in (0, 2\pi/3)$ satisfy $\theta_f/2 < \theta_c^\epsilon$ and $(r_D^S(s), \theta_D^S(s))$ parametrize the smooth solutions given by (22) and (23) terminating at $(\cos \theta_f, \sin \theta_f)$. By Propositions 4 and 5, θ_f and r_c are monotonically decreasing and increasing in D respectively, and thus $r_c(D(\theta_f)) \geq \epsilon$. Furthermore, since $r_D^S(s)$ is convex in s , it follows that $r_D^S(s) \geq \epsilon$ and thus $(r_D^S(s), \theta_D^S(s)) \in \mathcal{A}_\epsilon$. Finally, since $\mathcal{A}_\epsilon \subset \mathcal{A}_0$ and $(r_D^S(s), \theta_D^S(s))$ is assumed to minimize T over curves in \mathcal{A}_0 which terminate at $(\cos \theta_f, \sin \theta_f)$, it follows that $(r_D^S(s), \theta_D^S(s))$ also minimizes T over curves in \mathcal{A}_ϵ which terminate at $(\cos \theta_f, \sin \theta_f)$. □

For a strong solution given by (22) and (23) satisfying $\theta_f/2 > \theta_c^\epsilon$, let

$$s_D^\epsilon = \min\{(r_D^S)^{-1}\{\epsilon\}\},$$

i.e., the first point of intersection with the obstacle. The natural generalizations of Propositions 1 and 2 can be shown to hold for \mathcal{A}_ϵ and consequently we know, without loss of generality, that minimizers consist of curves symmetric about the angle $\theta_f/2$ that are smooth solutions given by (22) and (23) away from the constraint, ride along it for a finite amount of time, and then rejoin a rotated and reflected version of the latter half of the same smooth solution; see Figure 4. This family of minimizers is

$$\mathcal{F}_{D, \theta_f}^\epsilon(s) = \begin{cases} \left(r_D^S(h(s)) \cos(h(s)), r_D^S(h(s)) \sin(\theta_D^S(h(s))) \right), & s \in \left[0, \frac{1}{3} \right), \\ \left(\epsilon \cos(t(s)), \epsilon \sin(t(s)) \right) & s \in \left[\frac{1}{3}, \frac{2}{3} \right], \\ \left(r_D^S(s) \cos(l(s)), r_D^S(s) \sin(l(s)) \right) & s \in \left(\frac{2}{3}, 1 \right], \end{cases} \tag{35}$$

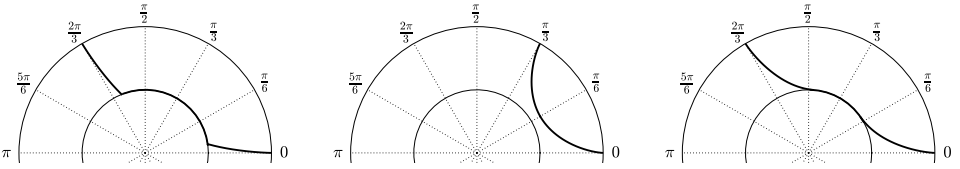


Figure 4. Plots of curves $\mathcal{F}_{D,\theta_f}^\epsilon(s)$ defined by (35) with $\epsilon = 0.5$. Left: a curve $\mathcal{F}_{D,\theta_f}^\epsilon(s)$ with $\theta_f = 2\pi/3$, $D = 0.0204$ and $\theta_c = \pi/4$ which reaches the obstacle and rides along it; (middle) a curve $\mathcal{F}_{D,\theta_f}^\epsilon(s)$ with $\theta_f = \pi/3$, $D = 0.2300$ and $\theta_c = \pi/6$ which does not reach the obstacle ($s_\epsilon = 0.5$); (right) a curve $\mathcal{F}_{D,\theta_f}^\epsilon(s)$ with $\theta_f = 2\pi/3$, $D = 0.1250$ and $\theta_c = 0.5981$ which approaches the obstacle at a tangent and rides along it.

where $r_D^S(s)$, $\theta_D^S(s)$ are given by (22) and (23) with $\theta_f(D)$ satisfying $\theta_f(D)/2 \geq \theta_c^\epsilon$,

$$\begin{aligned} h(s) &= s/(3s_D^\epsilon), & l(s) &= \theta_D^S(j_{D,\epsilon}(s)) + \theta_f - \theta_D^S(1), \\ j(s) &= 3s_D^\epsilon s + 1 - 3s_D^\epsilon, & t(s) &= 3(\theta_f - 2\theta^S(s_D^\epsilon))s + \theta_f - \theta^S(s_D^\epsilon). \end{aligned}$$

The following proposition characterizes the minimum of T over the family of curves given by (35); namely they consist of the curves defined by (35) that meet the constraint at a tangent.

Proposition 7. *Suppose that the smooth solution curves given by (22) and (23) are global minimizers in \mathcal{A}_0 . For $\epsilon > 0$, if $\theta_f/2 \geq \theta_c^\epsilon$ then the unique minimizer of T over the family of curves defined by (35) intersects the constraint tangentially.*

Proof. Let $\theta_f \in (0, \pi)$ satisfy $\theta_f/2 \geq \theta_c^\epsilon$. Let $\mathcal{F}_{D(\epsilon),\theta_f}^\epsilon(s)$ be the unique curve which intersects the constraint at a tangent and terminates at angular coordinate θ_f . Let $\mathcal{F}_{D,\theta_f}^\epsilon(s)$ be another curve with $D < D(\epsilon)$ that terminates at angular coordinate θ_f . By Propositions 4 and 5, θ_f and r_c are monotonically decreasing and increasing in D respectively; hence $r_c(D) \leq \epsilon$ and $\theta_c(D) \geq \theta_c^\epsilon$. Moreover, it follows from the monotonicity of $\theta_D^S(s)$ in s that $\mathcal{F}_{D,\theta_f}^\epsilon(s)$ intersects the constraint at some angular coordinate $\theta_0 < \theta_c^\epsilon$ and intersects $\mathcal{F}_{D(\epsilon),\theta_f}^\epsilon(s)$ at angular coordinate θ_c^ϵ . Since $\mathcal{F}_{D(\epsilon),\theta_f}^\epsilon(s)$ is of the form $(r_{D(\epsilon)}^S(s), \theta_{D(\epsilon)}^S(s))$ for $s < s_{D(\epsilon)}^\epsilon$, it follows from our assumption that smooth solutions given by (22) and (23) minimize T that $\mathcal{F}_{D(\epsilon),\theta_f}^\epsilon(s)$ minimizes the time of flight to angular coordinate θ_c^ϵ . Moreover, both curves have the same time of flight along the constraint from angular coordinates θ_c^ϵ to $\theta_f - \theta_c^\epsilon$, and consequently $T[\mathcal{F}_{D(\epsilon),\theta_f}^\epsilon(s)] < T[\mathcal{F}_{D,\theta_f}^\epsilon(s)]$. \square

4.3.1. Minimizers terminating on R_3 . Let $(r, \pi) \in R_3$. We know from our prior analysis in R_2 that all minimizers must ride along the obstacle until at least angular coordinate $\pi - \theta_c^\epsilon$. Hence, to minimize over curves terminating at (r, π) , we

need only minimize T over curves from $(\epsilon, \pi - \theta_c^\epsilon)$ to (r, π) . Note that from the convexity of strong solutions given by (22) and (23), there exists a unique angle $\phi_c^\epsilon \geq \pi - \theta_c^\epsilon$ such that the smooth solution comes off the obstacle tangentially at ϕ_c^ϵ and intersects (r, π) . It can be further shown that this curve minimizes the time of flight T between coordinates $(\epsilon, \pi - \theta_c^\epsilon)$ and (r, π) . This is made precise by the following proposition.

Proposition 8. *Suppose that the smooth solution curves given by (22) and (23) are global minimizers in \mathcal{A}_0 . For $\epsilon > 0$ and $(r, \pi) \in R_3$, a minimizer of T over \mathcal{A}_ϵ that terminates at (r, π) leaves the obstacle at a tangent.*

Proof. Let $\alpha^* \in \mathcal{A}_\epsilon$ denote the candidate minimizer that leaves the obstacle at a tangent from the angular coordinate ϕ_c^ϵ and terminates at the polar coordinate (r, π) . From the convexity of smooth solutions, we know that any other candidate minimizer $\alpha \in \mathcal{A}_\epsilon$ terminating at the polar coordinate (r, π) must come off the obstacle at some angular coordinate $\phi_0 > \phi_c^\epsilon$. Since the piece of the curve α^* that connects the polar coordinates $(\epsilon, \phi_c^\epsilon)$ to (r, π) is a smooth solution curve given by (22) and (23), it follows from our assumption that it minimizes the time of flight from polar coordinates $(\epsilon, \phi_c^\epsilon)$ to (r, π) . Consequently, the time of flight from polar coordinates (ϵ, ϕ_0) to (r, π) along α is larger.

Using the same method as in the proof of Proposition 7, it can be shown that it follows from our assumption that smooth solutions are given by (22) and (23), that a candidate minimizer coming off the obstacle at angular coordinate ϕ_0 has greater time of flight than one coming off at angular coordinate ϕ_c^ϵ . \square

4.3.2. Minimizers terminating on R_4 . Let $(\epsilon, \theta) \in R_4$. If $\theta < \theta_c^\epsilon$, there is a smooth solution given by (22) and (23) that, by assumption, minimizes the time of flight to (ϵ, θ) . If $\theta \in (\theta_c^\epsilon, \pi - \theta_c^\epsilon)$, there exists a curve in the family (35) that minimizes the time of flight to (ϵ, θ) . If $\theta > \theta_c^\epsilon$, it follows from Proposition 8 that there is a curve minimizing the time of flight that approaches the obstacle at a tangent and rides along until angular coordinate θ .

Remark. The solution curves connected to the boundary foliate the domain. Specifically, there are three distinct areas A_1, A_2 and A_3 satisfying $\mathcal{O}_\epsilon = A_1 \cup A_2 \cup A_3$ that are foliated by curves connected to the boundary in R_2, R_3 and R_4 respectively. This is illustrated in Figure 5.

4.4. Convergence to weak solutions. In the previous section, Propositions 6 and 7 describe the behavior of a family of curves that minimizes T to terminal polar coordinates $(1, \theta_f) \in R_2$. For a given value of $\epsilon \in (0, 1)$ and $\theta_f \in (0, \pi)$, we denote this family as

$$\alpha_{\theta_f}^\epsilon(s) = \begin{cases} (r_{D(\theta_f)}^S(s) \cos(\theta_{D(\theta_f)}^S(s)), r_{D(\theta_f)}^S(s) \sin(\theta_{D(\theta_f)}^S(s))) & \text{if } \theta_f/2 \leq \theta_c^\epsilon, \\ \mathcal{F}_{D(\epsilon), \theta_f}^\epsilon(s) & \text{if } \theta_f/2 > \theta_c^\epsilon, \end{cases} \quad (36)$$

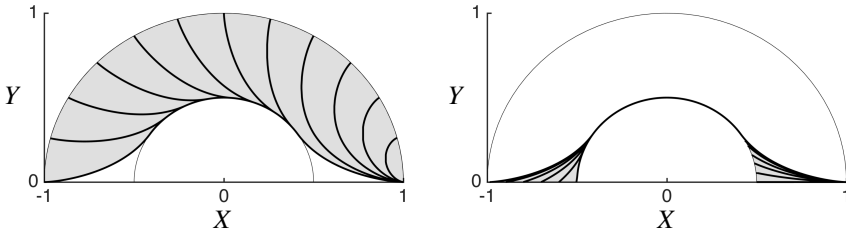


Figure 5. Left: The annulus \mathcal{O}_ϵ with A_1 shaded in. A_1 consists of the set of points which lie on solution curves terminating on R_2 . Overlaid on A_1 are evenly spaced solution curves terminating on R_2 given by (35). Right: The annulus \mathcal{O}_ϵ with A_2, A_3 shaded in. A_2 and A_3 consist of the sets of points which lie on solution curves terminating on R_3 and R_4 respectively. Overlaid on A_2 and A_3 are evenly spaced solution curves terminating in R_3 and R_4 .

where $(r_{D(\theta_f)}^S(s), \theta_{D(\theta_f)}^S(s))$ are the radial and angular coordinates of the unique smooth solution given by (22) and (23), and $\mathcal{F}_{D(\epsilon), \theta_f}^\epsilon(s)$ is a member of the family described by (35). Moreover, as ϵ approaches 0, this family converges to the natural foliation of the unit disk described in Figure 3 (right) and given by

$$\alpha_{\theta_f}(s) = \begin{cases} (r_{D(\theta_f)}^S(s) \cos(\theta_{D(\theta_f)}^S(s)), r_{D(\theta_f)}^S(s) \sin(\theta_{D(\theta_f)}^S(s))) & \text{if } \theta_f < 2\pi/3, \\ (r^W(s) \cos(\theta^W(s)), r^W(s) \sin(\theta^W(s))) & \text{if } \theta_f \geq 2\pi/3, \end{cases} \quad (37)$$

where $r^W(s), \theta^W(s)$ are the radial and angular coordinates of the unique smooth solution given by (25) and (26) with $|B| = 1$ and θ_f . This is made precise in the following proposition.

Proposition 9. For $\theta_f \in (0, \pi)$,

$$\lim_{\epsilon \rightarrow 0} d(\alpha_{\theta_f}^\epsilon, \alpha_{\theta_f}) = 0,$$

where

$$d(\alpha_{\theta_f}, \alpha_{\theta_f}) = \sup_{0 \leq s \leq 1} \inf_{0 \leq t \leq 1} |\alpha_{\theta_f}^\epsilon(s) - \alpha_{\theta_f}(t)|$$

is the natural distance between the images of curves in the uniform norm.

Proof. Let $\theta_f \in (0, \pi)$ and define the sequence of functions $\alpha_{\theta_f}^\epsilon(s)$ by (36).

(1) If $\theta_f < 2\pi/3$, there exists some $D(\theta_f) > 0$ such that the smooth solution $(r_{D(\theta_f)}^S(s), \theta_{D(\theta_f)}^S(s))$ given by (22) and (23) terminates at $(1, \theta_f)$. By Proposition 5,

$$\lim_{\epsilon \rightarrow 0} \theta_c^\epsilon = \pi/3 \geq \theta_f/2.$$

Therefore, there exists ϵ^* such that $\epsilon < \epsilon^* \implies \alpha_{\theta_f}^\epsilon = \alpha_{\theta_f}$. Thus, for $\theta_f < 2\pi/3$,

$$\lim_{\epsilon \rightarrow 0} d(\alpha_{\theta_f}^\epsilon, \alpha_{\theta_f}) = 0.$$

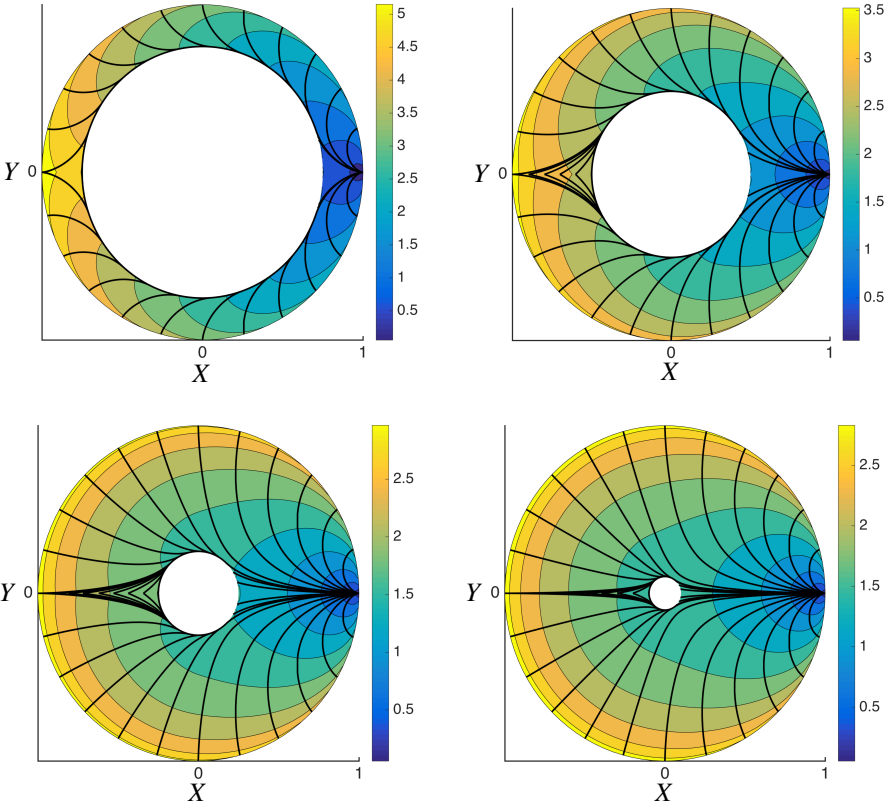


Figure 6. A foliation of the annuli $\mathcal{O}_{0.75}$, $\mathcal{O}_{0.5}$, $\mathcal{O}_{0.25}$, $\mathcal{O}_{0.1}$ by evenly spaced solution curves terminating on the boundary of the annulus. Beneath the solution curves of each subfigure is a contour plot of the time of flight from $(1, 0)$ to each point on the annulus by solution curves of the form given by (36).

(2) If $\theta_f \geq 2\pi/3$, then $\alpha_{\theta_f}^\epsilon$ approaches the obstacle tangentially at (r, ϵ_c^ϵ) along the path of a smooth solution for $s \in [0, 1/3]$. It follows from the convexity of smooth solutions that $\alpha_{\theta_f}^\epsilon([0, 1/3])$ is contained in the rectangular region

$$\mathcal{R}_\epsilon = \{(x, y) \in \mathbb{R}^2 : x \in [\epsilon \cos(\theta_c^\epsilon), 1], y \in [0, \epsilon \sin(\theta_c^\epsilon)]\}.$$

As $\epsilon \rightarrow 0$, the region \mathcal{R}_ϵ limits to the line $\{(x, y) \in \mathbb{R}^2 : x \in [0, 1], y = 0\}$. Moreover, $\alpha_{\theta_f}^\epsilon([1/3, 2/3])$ is on the obstacle and consequently limits to the origin as $\epsilon \rightarrow 0$. It follows immediately from radial symmetry that a rotated rectangular region can be constructed around $\alpha_{\theta_f}^\epsilon([2/3, 1])$ that limits to the line $\theta = \theta_f$. Hence each point on $\alpha_{\theta_f}^\epsilon$ limits to a point along the weak solution $(r^W(s) \cos(\theta^W(s)), r^W(s) \sin(\theta^W(s)))$ and thus for $\theta_f > 2\pi/3$,

$$\lim_{\epsilon \rightarrow 0} d(\alpha_{\theta_f}^\epsilon, \alpha_{\theta_f}) = 0.$$

□

The solution curves depicted in [Figure 6](#) again intersect the level sets of the value function orthogonally. This is consistent with [\(13\)](#); i.e., \mathcal{V} satisfies the eikonal equation defined by [\(12\)](#) on an annular domain.

5. Discussion and conclusion

In this paper we solved the brachistochrone problem in the inverse-square gravitational field. Namely, we constructed solutions that enter the so-called forbidden region first mentioned in [[Parnovsky 1998](#); [Tee 1999](#); [Gemmer et al. 2011](#)]. Furthermore we considered the constrained problem where solutions are restricted to lie outside of a ball around the origin. This restricted problem is more physically relevant since it avoids the particle experiencing infinite acceleration at the origin. Moreover, the solutions in the annular domain recover our prior solutions on the disk in the limit of vanishing inner radius. Consequently these solutions on the annular domain correspond to “regularized” brachistochrone solutions that avoid the singularity.

In the future, this work could be extended to problems with multiple singularities. That is, a natural extension of this work is to consider brachistochrone problems with multiple point sources of gravity. Natural questions to consider would be what role if any does the existence of a forbidden region play in the selection of strong or weak solutions. If weak solutions do exist, we conjecture that they would form a network of strong solutions patched together at singularities of the gravitational field. We expect that many of our results would hold locally near a singularity. However, by adding multiple singularities we break the radial invariance which we exploited to explicitly construct global solutions.

We also should mention that we have only considered necessary conditions for optimality. Specifically, this problem is not completely solved in the modern sense without a proof of the existence of a minimizer. This is not a trivial task since the functional is not coercive and is not convex at the singular origin and hence the direct method of the calculus of variations cannot be applied. We conjecture that the general results for noncoercive integrals presented in [[Botteron and Marcellini 1991](#)] or the technique of convex rearrangement presented in [[Greco 2012](#)] can be adapted to prove existence on the annular domain. Consequently, we expect that we could prove an existence result on the entire disk by considering the limit of vanishing inner radius.

Acknowledgments

We wish to acknowledge Zachary Nado for many fruitful conversations. Grimm would also like to thank the MAA for providing travel support to attend MathFest 2015, where this work was first presented. Gemmer is currently supported by NSF-RTG grant DMS-1148284.

References

- [Audoly and Boudaoud 2003] B. Audoly and A. Boudaoud, “Self-similar structures near boundaries in strained systems”, *Phys. Rev. Lett.* **91** (Aug 2003), art. id. 086105, 4 pp.
- [Bertsekas 1995] D. P. Bertsekas, *Dynamic programming and optimal control*, vol. 1, Athena Scientific, Belmont, MA, 1995. [MR](#) [Zbl](#)
- [Bhattacharya 2003] K. Bhattacharya, *Microstructure of martensite: why it forms and how it gives rise to the shape-memory effect*, Oxford Series on Materials Modelling **2**, Oxford University Press, 2003. [MR](#) [Zbl](#)
- [Blåsjö 2005] V. Blåsjö, “The isoperimetric problem”, *Amer. Math. Monthly* **112**:6 (2005), 526–566. [MR](#) [Zbl](#)
- [Botteron and Marcellini 1991] B. Botteron and P. Marcellini, “A general approach to the existence of minimizers of one-dimensional non-coercive integrals of the calculus of variations”, *Ann. Inst. H. Poincaré Anal. Non Linéaire* **8**:2 (1991), 197–223. [MR](#) [Zbl](#)
- [Broer 2014] H. W. Broer, “Bernoulli’s light ray solution of the brachistochrone problem through Hamilton’s eyes”, *Internat. J. Bifur. Chaos Appl. Sci. Engrg.* **24**:8 (2014), art. id. 1440009, 15 pp. [MR](#) [Zbl](#)
- [DeSimone et al. 2000] A. DeSimone, R. V. Kohn, S. Müller, and F. Otto, “Magnetic microstructures: a paradigm of multiscale problems”, pp. 175–190 in *ICIAM 99: proceedings of the Fourth International Congress on Industrial and Applied Mathematics* (Edinburgh, 1999), edited by J. M. Ball and J. C. R. Hunt, Oxford Univ. Press, 2000. [MR](#) [Zbl](#)
- [Dunham 1990] W. Dunham, *Journey through genius: the great theorems of mathematics*, Wiley, New York, 1990. [MR](#) [Zbl](#)
- [Erlichson 1999] H. Erlichson, “Johann Bernoulli’s brachistochrone solution using Fermat’s principle of least time”, *European J. Phys.* **20**:5 (1999), 299–304. [MR](#) [Zbl](#)
- [Evans 1998] L. C. Evans, *Partial differential equations*, Graduate Studies in Mathematics **19**, American Mathematical Society, Providence, RI, 1998. [MR](#) [Zbl](#)
- [Gemmer et al. 2011] J. A. Gemmer, M. Nolan, and R. Umble, “Generalizations of the brachistochrone problem”, *Pi Mu Epsilon Journal* **13**:4 (2011), 207–218.
- [Gemmer et al. 2016] J. Gemmer, E. Sharon, T. Shearman, and S. C. Venkataramani, “Isometric immersions, energy minimization and self-similar buckling in non-Euclidean elastic sheets”, *Europhys. Lett.* **114**:2 (2016), art. id. 24003, 6 pp.
- [Goldstein et al. 2014] H. Goldstein, C. P. Poole, and J. L. Safko, *Classical mechanics*, 3rd ed., Pearson, Harlow, 2014.
- [Greco 2012] A. Greco, “Minimization of non-coercive integrals by means of convex rearrangement”, *Adv. Calc. Var.* **5**:2 (2012), 231–249. [MR](#) [Zbl](#)
- [Kohn 2007] R. V. Kohn, “Energy-driven pattern formation”, pp. 359–383 in *International Congress of Mathematicians* (Madrid, 2006), vol. 1, edited by M. Sanz-Solé et al., Eur. Math. Soc., Zürich, 2007. [MR](#) [Zbl](#)
- [Leoni 2009] G. Leoni, *A first course in Sobolev spaces*, Graduate Studies in Mathematics **105**, American Mathematical Society, Providence, RI, 2009. [MR](#) [Zbl](#)
- [McCleary 2013] J. McCleary, *Geometry from a differentiable viewpoint*, 2nd ed., Cambridge University Press, 2013. [MR](#) [Zbl](#)
- [Müller 1999] S. Müller, “Variational models for microstructure and phase transitions”, pp. 85–210 in *Calculus of variations and geometric evolution problems* (Cetraro, 1996), edited by S. Hildebrandt and M. Struwe, Lecture Notes in Math. **1713**, Springer, 1999. [MR](#) [Zbl](#)

- [Nakane and Fraser 2002] M. Nakane and C. G. Fraser, “The early history of Hamilton–Jacobi dynamics 1834–1837”, *Centaurus* **44**:3-4 (2002), 161–227. [MR](#) [Zbl](#)
- [Oprea 2000] J. Oprea, *The mathematics of soap films: explorations with Maple*, Student Mathematical Library **10**, American Mathematical Society, Providence, RI, 2000. [MR](#) [Zbl](#)
- [Ortiz and Gioia 1994] M. Ortiz and G. Gioia, “The morphology and folding patterns of buckling-driven thin-film blisters”, *J. Mech. Phys. Solids* **42**:3 (1994), 531–559. [MR](#) [Zbl](#)
- [Parnovsky 1998] A. Parnovsky, “Some generalisations of brachistochrone problem”, *Acta Physica Polonica A* **93**:Supplement (1998), S–55.
- [Royden and Fitzpatrick 2010] H. Royden and P. Fitzpatrick, *Real analysis*, 4th ed., Pearson, Boston, 2010. [Zbl](#)
- [Sagan 1969] H. Sagan, *Introduction to the calculus of variations*, McGraw-Hill, New York, 1969. Reprinted Dover, New York, 1992. [MR](#)
- [Sharon et al. 2007] E. Sharon, B. Roman, and H. L. Swinney, “Geometrically driven wrinkling observed in free plastic sheets and leaves”, *Phys. Rev. E* **75**:4 (2007), art. id. 046211, 7 pp.
- [Song et al. 2008] J. Song, H. Jiang, W. M. Choi, D. Y. Khang, Y. Huang, and J. A. Rogers, “An analytical study of two-dimensional buckling of thin films on compliant substrates”, *J. Appl. Phys.* **103**:1 (2008), art. id. 014303, 10 pp.
- [Sussmann and Willems 1997] H. J. Sussmann and J. C. Willems, “300 years of optimal control: from the brachistochrone to the maximum principle”, *IEEE Control Systems* **17**:3 (1997), 32–44.
- [Tee 1999] G. J. Tee, “Isochrones and brachistochrones”, *Neural Parallel Sci. Comput.* **7**:3 (1999), 311–341. [MR](#) [Zbl](#)
- [Witten 2007] T. A. Witten, “Stress focusing in elastic sheets”, *Rev. Modern Phys.* **79**:2 (2007), 643–675. [MR](#) [Zbl](#)

Received: 2016-05-05 Accepted: 2016-07-24

christopher_grimm@brown.edu *Department of Computer Science, Brown University,
Providence, RI 02912, United States*

gemmerj@wfu.edu *Department of Mathematics, Wake Forest University,
Winston Salem, NC 27109, United States*

INVOLVE YOUR STUDENTS IN RESEARCH

Involve showcases and encourages high-quality mathematical research involving students from all academic levels. The editorial board consists of mathematical scientists committed to nurturing student participation in research. Bridging the gap between the extremes of purely undergraduate research journals and mainstream research journals, *Involve* provides a venue to mathematicians wishing to encourage the creative involvement of students.

MANAGING EDITOR

Kenneth S. Berenhaut Wake Forest University, USA

BOARD OF EDITORS

Colin Adams	Williams College, USA	Suzanne Lenhart	University of Tennessee, USA
John V. Baxley	Wake Forest University, NC, USA	Chi-Kwong Li	College of William and Mary, USA
Arthur T. Benjamin	Harvey Mudd College, USA	Robert B. Lund	Clemson University, USA
Martin Bohner	Missouri U of Science and Technology, USA	Gaven J. Martin	Massey University, New Zealand
Nigel Boston	University of Wisconsin, USA	Mary Meyer	Colorado State University, USA
Amarjit S. Budhiraja	U of North Carolina, Chapel Hill, USA	Emil Minchev	Ruse, Bulgaria
Pietro Cerone	La Trobe University, Australia	Frank Morgan	Williams College, USA
Scott Chapman	Sam Houston State University, USA	Mohammad Sal Moslehian	Ferdowsi University of Mashhad, Iran
Joshua N. Cooper	University of South Carolina, USA	Zuhair Nashed	University of Central Florida, USA
Jem N. Corcoran	University of Colorado, USA	Ken Ono	Emory University, USA
Toka Diagana	Howard University, USA	Timothy E. O'Brien	Loyola University Chicago, USA
Michael Dorff	Brigham Young University, USA	Joseph O'Rourke	Smith College, USA
Sever S. Dragomir	Victoria University, Australia	Yuval Peres	Microsoft Research, USA
Behrouz Emamizadeh	The Petroleum Institute, UAE	Y.-F. S. Pétermann	Université de Genève, Switzerland
Joel Foisy	SUNY Potsdam, USA	Robert J. Plemmons	Wake Forest University, USA
Erin W. Fulp	Wake Forest University, USA	Carl B. Pomerance	Dartmouth College, USA
Joseph Gallian	University of Minnesota Duluth, USA	Vadim Ponomarenko	San Diego State University, USA
Stephan R. Garcia	Pomona College, USA	Bjorn Poonen	UC Berkeley, USA
Anant Godbole	East Tennessee State University, USA	James Propp	U Mass Lowell, USA
Ron Gould	Emory University, USA	József H. Przytycki	George Washington University, USA
Andrew Granville	Université Montréal, Canada	Richard Rebarber	University of Nebraska, USA
Jerrold Griggs	University of South Carolina, USA	Robert W. Robinson	University of Georgia, USA
Sat Gupta	U of North Carolina, Greensboro, USA	Filip Saidak	U of North Carolina, Greensboro, USA
Jim Haglund	University of Pennsylvania, USA	James A. Sellers	Penn State University, USA
Johnny Henderson	Baylor University, USA	Andrew J. Sterge	Honorary Editor
Jim Hoste	Pitzer College, USA	Ann Trenk	Wellesley College, USA
Natalia Hritonenko	Prairie View A&M University, USA	Ravi Vakil	Stanford University, USA
Glenn H. Hurlbert	Arizona State University, USA	Antonia Vecchio	Consiglio Nazionale delle Ricerche, Italy
Charles R. Johnson	College of William and Mary, USA	Ram U. Verma	University of Toledo, USA
K. B. Kulasekera	Clemson University, USA	John C. Wierman	Johns Hopkins University, USA
Gerry Ladas	University of Rhode Island, USA	Michael E. Zieve	University of Michigan, USA

PRODUCTION

Silvio Levy, Scientific Editor


Cover: Alex Scorpan

See inside back cover or msp.org/involve for submission instructions. The subscription price for 2017 is US \$175/year for the electronic version, and \$235/year (+\$35, if shipping outside the US) for print and electronic. Subscriptions, requests for back issues and changes of subscriber address should be sent to MSP.

Involve (ISSN 1944-4184 electronic, 1944-4176 printed) at Mathematical Sciences Publishers, 798 Evans Hall #3840, c/o University of California, Berkeley, CA 94720-3840, is published continuously online. Periodical rate postage paid at Berkeley, CA 94704, and additional mailing offices.

Involve peer review and production are managed by EditFLOW® from Mathematical Sciences Publishers.

PUBLISHED BY

 **mathematical sciences publishers**
nonprofit scientific publishing

<http://msp.org/>

© 2017 Mathematical Sciences Publishers

involve

2017

vol. 10

no. 5

Algorithms for finding knight's tours on Aztec diamonds	721
SAMANTHA DAVIES, CHENXIAO XUE AND CARL R. YERGER	
Optimal aggression in kleptoparasitic interactions	735
DAVID G. SYKES AND JAN RYCHTÁŘ	
Domination with decay in triangular matchstick arrangement graphs	749
JILL COCHRAN, TERRY HENDERSON, AARON OSTRANDER AND RON TAYLOR	
On the tree cover number of a graph	767
CHASSIDY BOZEMAN, MINERVA CATRAL, BRENDAN COOK, OSCAR E. GONZÁLEZ AND CAROLYN REINHART	
Matrix completions for linear matrix equations	781
GEOFFREY BUHL, ELIJAH CRONK, ROSA MORENO, KIRSTEN MORRIS, DIANNE PEDROZA AND JACK RYAN	
The Hamiltonian problem and t -path traceable graphs	801
KASHIF BARI AND MICHAEL E. O'SULLIVAN	
Relations between the conditions of admitting cycles in Boolean and ODE network systems	813
YUNJIAO WANG, BAMIDELE OMIDIRAN, FRANKLIN KIGWE AND KIRAN CHILAKAMARRI	
Weak and strong solutions to the inverse-square brachistochrone problem on circular and annular domains	833
CHRISTOPHER GRIMM AND JOHN A. GEMMER	
Numerical existence and stability of steady state solutions to the distributed spruce budworm model	857
HALA AL-KHALIL, CATHERINE BRENNAN, ROBERT DECKER, ASLIHAN DEMIRKAYA AND JAMIE NAGODE	
Integer solutions to $x^2 + y^2 = z^2 - k$ for a fixed integer value k	881
WANDA BOYER, GARY MACGILLIVRAY, LAURA MORRISON, C. M. (KIEKA) MYNHARDT AND SHAHLA NASSERASR	
A solution to a problem of Frechette and Locus	893
CHENTHURAN ABEYAKARAN	